

Supporting information

Synergistic Effect of Pseudo-Halide Thiocyanate Anion and Cesium Cation on Realizing High-Performance Pinhole Free MA-Based Wide-Band Gap Perovskites

Yue-Min Xie,^{†,‡,§} Xiuwen Xu,^{†,‡,§} Chunqing Ma,[‡] Menglin Li,^{†,‡,§} Yuhui Ma^{†,‡,§} Chun-Sing Lee,[‡] and Sai-Wing Tsang^{,†,‡,§}*

[†]Department of Materials Science and Engineering and [‡]Center of Super-Diamond and Advanced Films (COSDAF), City University of Hong Kong, Kowloon, Hong Kong SAR, P. R. China

[§]City University of Hong Kong Shenzhen Research Institute, Shenzhen 518057, P. R. China

Corresponding Author

* E-mail: saitsang@cityu.edu.hk

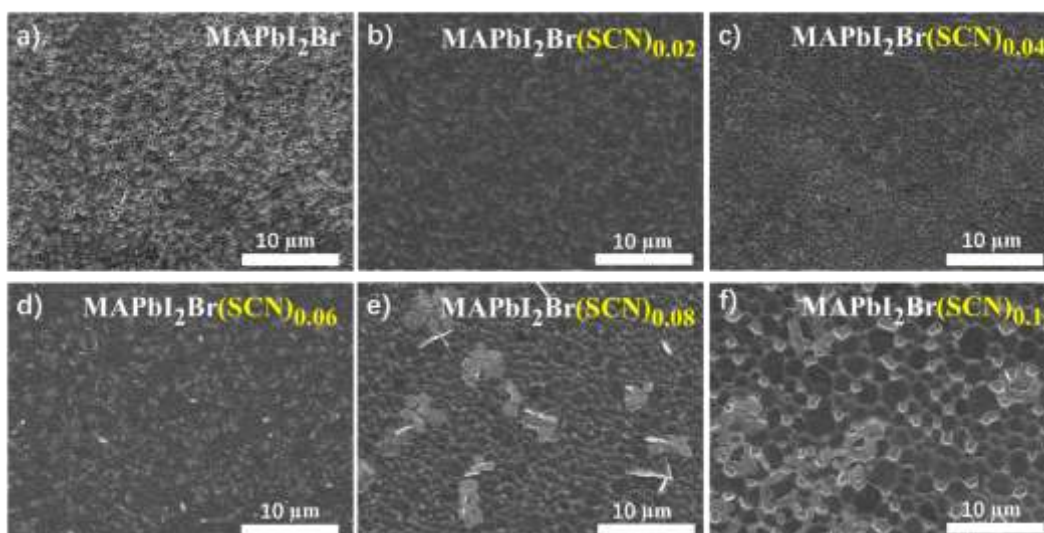


Figure S1. Large-scale SEM images of MAPbI₂Br perovskites with the Pb(SCN)₂ additive ratio of a) 0, b) 1%, c) 2%, d) 3%, e) 4% and f) 5%, respectively.

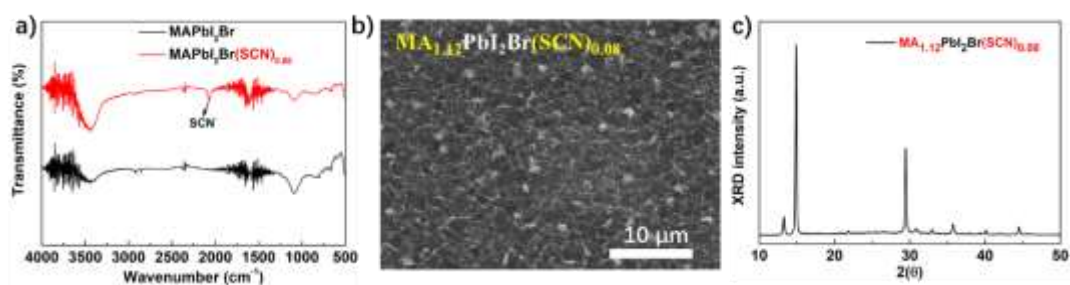


Figure S2. a) FTIR spectra of MAPbI₂Br and MAPbI₂Br(SCN)_{0.08}, respectively. b-c) SEM and XRD results of film prepared with precursor solution of MA_{1.12}PbI₂Br(SCN)_{0.08}.

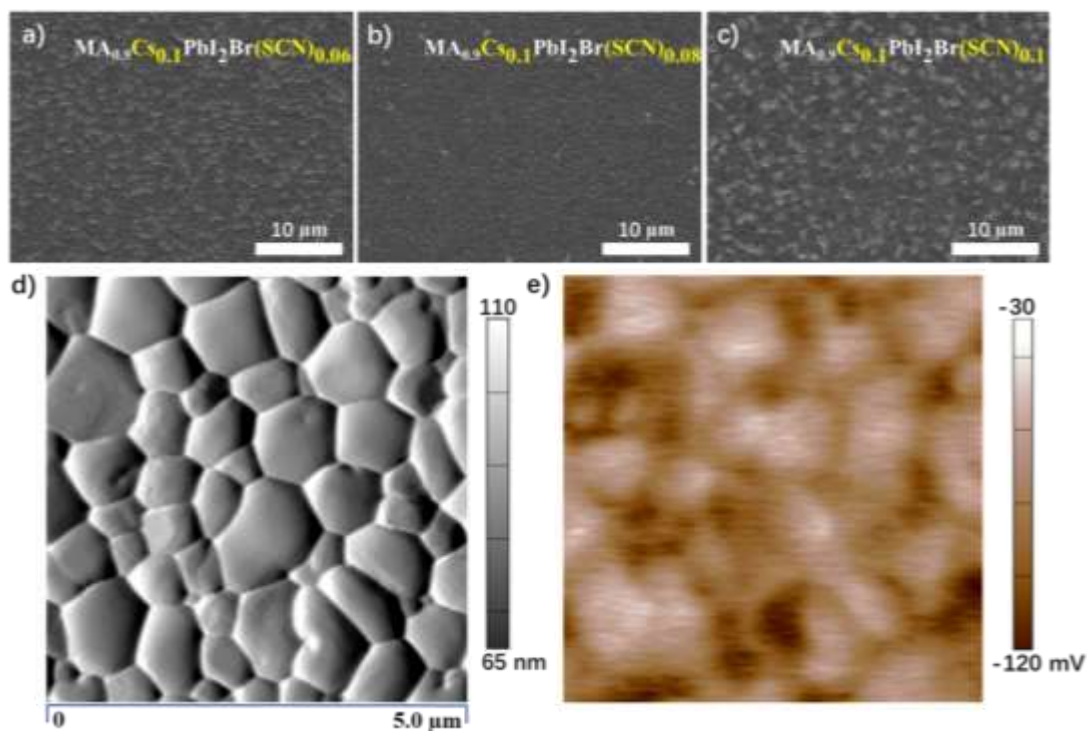


Figure S3. a-c) Large-scale SEM images of perovskite film prepared with precursor solution of $\text{MA}_{0.9}\text{Cs}_{0.1}\text{PbI}_2\text{Br}(\text{SCN})_{0.06}$, $\text{MA}_{0.9}\text{Cs}_{0.1}\text{PbI}_2\text{Br}(\text{SCN})_{0.08}$ and $\text{MA}_{0.9}\text{Cs}_{0.1}\text{PbI}_2\text{Br}(\text{SCN})_{0.1}$, respectively. d) AFM topography and e) the contact potential difference (CPD) maps of film $\text{MA}\text{PbI}_2\text{Br}(\text{SCN})_{0.08}$.

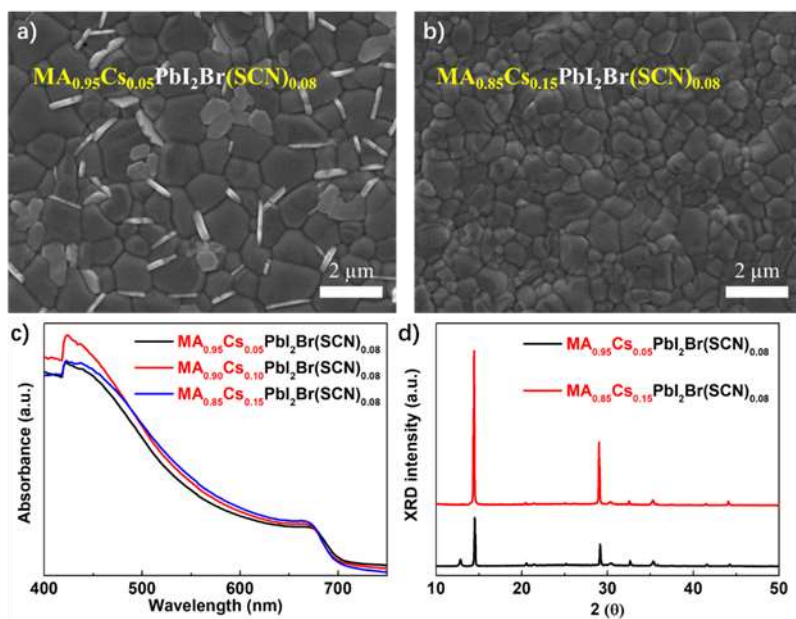


Figure S4. SEM images of perovskite films prepared with precursor solution of a) $\text{MA}_{0.95}\text{Cs}_{0.05}\text{PbI}_2\text{Br}(\text{SCN})_{0.08}$ and b) $\text{MA}_{0.85}\text{Cs}_{0.15}\text{PbI}_2\text{Br}(\text{SCN})_{0.08}$, respectively. c-d) UV-Vis absorption results of perovskite films prepared with precursor solution of $\text{MA}_{0.95}\text{Cs}_{0.05}\text{PbI}_2\text{Br}(\text{SCN})_{0.08}$, $\text{MA}_{0.90}\text{Cs}_{0.10}\text{PbI}_2\text{Br}(\text{SCN})_{0.08}$ and $\text{MA}_{0.85}\text{Cs}_{0.15}\text{PbI}_2\text{Br}(\text{SCN})_{0.08}$, respectively. d) XRD results of the films prepared with precursor solution of $\text{MA}_{0.95}\text{Cs}_{0.05}\text{PbI}_2\text{Br}(\text{SCN})_{0.08}$ and $\text{MA}_{0.85}\text{Cs}_{0.15}\text{PbI}_2\text{Br}(\text{SCN})_{0.08}$, respectively.

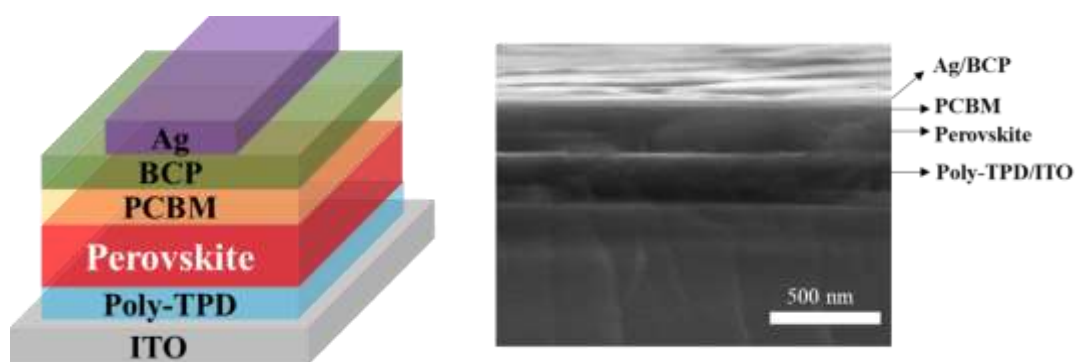


Figure S5. Device structure and corresponding cross-section SEM image of the perovskite solar cells in this work.

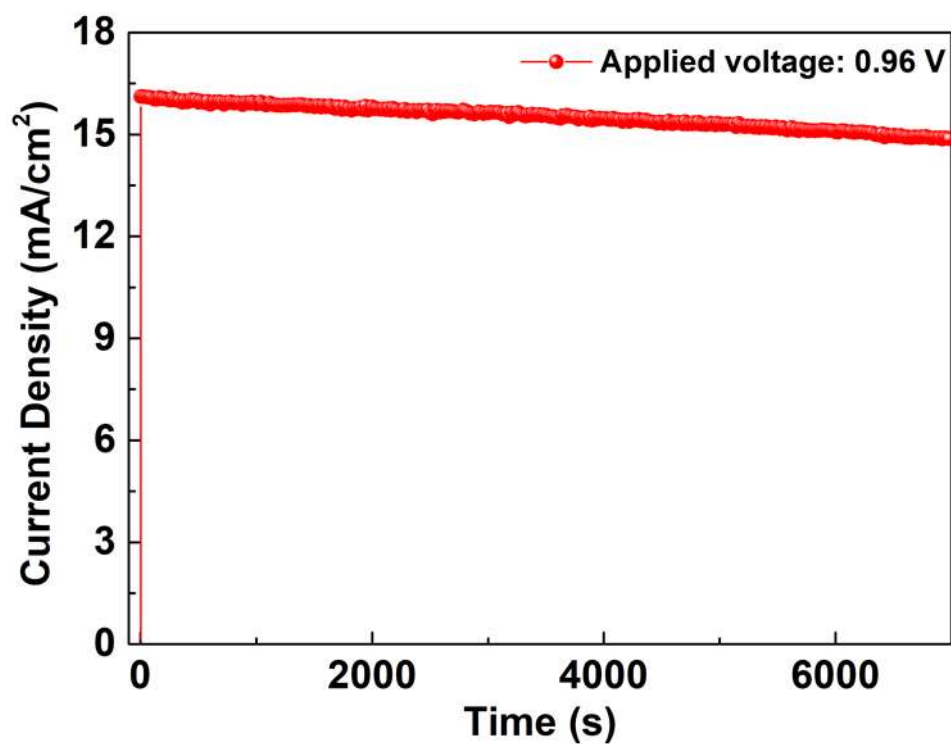


Figure S6. Steady-state current density (J_{sc}) under AM1.5 illumination at the applied voltage corresponding to the maximum power point (0.96 V) tested under ambient atmosphere without encapsulation.

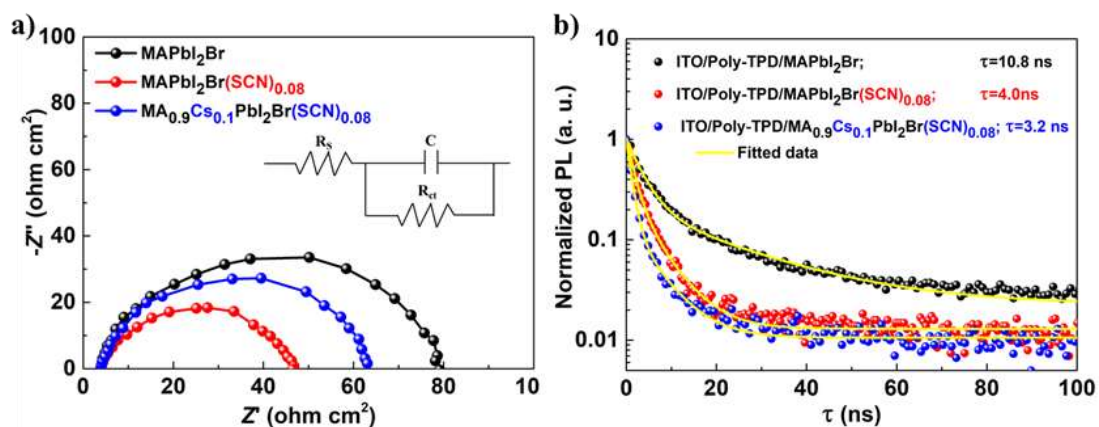


Figure S7. EIS spectra of MA_{0.9}CS_{0.1}PbI₂Br(SCN)_{0.08}, MA_{0.9}CS_{0.1}PbI₂Br(SCN)_{0.08} and MA_{0.9}CS_{0.1}PbI₂Br(SCN)_{0.08} based PVSCs measured at open circuit condition ($V = 1.04$, 1.12 and 1.15 V, respectively).